Dimerization and Inter-Chromophore Distance of Cph1 Phytochrome from *Synechocystis*, as Monitored by Fluorescence Homo and Hetero Energy Transfer[†]

Harald Otto,*[,‡] Tilman Lamparter,[§] Berthold Borucki,[‡] Jon Hughes,[||] and Maarten P. Heyn*[,‡]

Biophysics Group, Department of Physics, Freie Universität Berlin, Arnimallee 14, D-14195 Berlin, Germany, Plant Physiology, Department of Biology, Freie Universität Berlin, Königin-Luise-Strasse 12, D-14195 Berlin, Germany, and Plant Physiology, Department of Biology, Justus-Liebig Universität Giessen, Senckenbergstrasse 3, D-35390 Giessen, Germany

Received October 3, 2002; Revised Manuscript Received February 24, 2003

ABSTRACT: We investigated the dimerization of phytochrome Cph1 from the cyanobacterium *Synechocystis* by fluorescence resonance energy transfer (FRET). As donor we used the chromophore analogue phycoerythrobilin (PEB) and as acceptor either the natural chromophore phycocyanobilin (PCB; hetero transfer) or PEB (homo transfer). Both chromophores bind in a 1:1 stoichiometry to apo-monomers expressed in *Escherichia coli*. Energy transfer was characterized by time-resolved fluorescence intensity and anisotropy decay after excitation of PEB by picosecond pulses from a tunable Ti-sapphire laser system. ApoCph1 was first assembled with PEB at a low stoichiometry of 0.1. The remaining sites were then sequentially titrated with PCB. In the course of this titration, the mean lifetime of PEB decreased from 3.33 to 1.25 ns in the P_r form of Cph1, whereas the anisotropy decay was unaffected. In the P_{fr}/P_r photoequilibrium (about 65% P_{fr}), the mean lifetime decreased significantly less, to 1.67 ns. These observations provide strong support for inter-chromophore hetero energy transfer in mixed PEB/PCB dimers. The reduced energy transfer in P_{fr} may be due to a structural difference but is at least in part due to the difference in spectral overlap, which was 4.1×10^{-13} and 1.6×10^{-13} cm^3 M^{-1} in P_r and P_{fr}, respectively. From the changes in the mean lifetime, rates of hetero energy transfer of 0.68 and 0.37 ns^{-1} were calculated for the P_r form and the P_{fr}/P_r photoequilibrium, respectively. Sequential titration of apo Cph1 with PEB alone to full occupancy did not affect the intensity decay but led to a substantial increase in depolarization. This is the experimental signature of homo energy transfer. Values for the rate of energy transfer k_{HT} (0.47 ns^{-1}) and the angle 2θ between the transition dipole moment directions ($2\theta = 45 \pm 5°$) were determined from an analysis of the concentration dependence of the anisotropy at five different PEB/Cph1 stoichiometries. The independently determined rates of hetero and homo energy transfer are thus of comparable magnitude and consistent with the energy transfer interpretation. Using these results and exploiting the 2-fold symmetry of the dimer, the chromophore−chromophore distance R_{DA} was calculated and found to be in the range 49 Å < R_{DA} < 63 Å. Further evidence for energy transfer in Cph1 dimers was obtained from dilution experiments with PEB/PEB dimers: the lifetime was unchanged, but the anisotropy increased as the dimers dissociated with increasing dilution. These experiments allowed a rough estimate of 5 ± 3 μM for the dimer dissociation constant. With the deletion mutant Cph1Δ2 that lacks the carboxy terminal histidine kinase domain less energy transfer was observed suggesting that in this mutant dimerization is much weaker. The carboxy terminal domain of Cph1 that is involved in intersubunit trans-phosphorylation and signal transduction thus plays a dominant role in the dimerization. The FRET method provides a sensitive assay to monitor the association of Cph1 monomers.

Phytochromes are photoreceptors of plants but have recently also been discovered in prokaryotes (*1*−*5*). Here, we investigated the phytochrome Cph1 from the cyanobacterium *Synechocystis* PCC 6803 (for a review see ref *6*). The apo protein was expressed in *Escherichia coli* and assembled in vitro with the linear tetrapyrroles phycocyanobilin (PCB),[1] phycoerythrobilin (PEB), and phytochromobilin (PΦB). Upon autocatalytic assembly with PCB, P_r is formed with an absorption maximum at 656 nm; this form photoconverts into P_{fr}, which absorbs maximally at 702 nm (*7*). The transition between P_r and P_{fr} is photoreversible with about 65% P_{fr} in the photoequilibrium induced by red light (∼650 nm) and is associated with an isomerization around the C_{15}═C_{16} double bond of the bilin chromophore. The holo protein

[†] This research was supported by grants from the Deutsche Forschungsgemeinschaft (Sfb 498) to M.P.H., T.L., and J.H.

* To whom correspondence should be addressed. (H.O.) E-mail: otto@physik.fu-berlin.de. (M.P.H.) E-mail: heyn@physik.fu-berlin.de. Fax: ++49-30-838 56 299.

[‡] Department of Physics, Freie Universität Berlin.

[§] Department of Biology, Freie Universität Berlin.

[||] Justus-Liebig Universität Giessen.

[1] Abbreviations: PCB, phycocyanobilin; PEB, phycoerythrobilin; PΦB, phytochromobilin; P_r, red absorbing form of phytochrome; P_{fr}, far-red absorbing form of phytochrome; Cph1, cyanobacterial phytochrome from *Synechocystis*; Cph1Δ2, N-terminal chromophore carrying domain of Cph1 lacking the histidine kinase domain; FRET, fluorescence resonance energy transfer; PAS, acronym formed from the names of the first three proteins recognized as sharing this sensory domain; SEC, size-exclusion chromatography; Rcp1, response regulator for cyanobacterial phytochrome.

10.1021/bi026946y CCC: $25.00
Published on Web 04/23/2003

has been characterized by flash spectroscopy (*8*, *9*), resonance Raman spectroscopy (*8*), Fourier transform infrared spectroscopy (*10*), and fluorescence spectroscopy (*11*, *12*). These experiments indicate that there are substantial similarities between Cph1 and plant phytochromes. The transition between P_r and P_{fr} is also accompanied by light-induced release and uptake of protons, which is probably due to p*K* changes induced by structural changes (*9*). Cph1 is a light-regulated histidine kinase of the two-component type (*2*), which interacts with the response regulator Rcp1 (*2*). The histidine kinase activity is greater in P_r than in P_{fr} (*2*). Cph1 can be expressed in *E. coli* at high yield and is an excellent model system to study the mechanism of signal transduction within the phytochrome molecule. The natural chromophore of Cph1 is PCB (*13*). As in plant phytochrome (*14*, *15*), the PCB adduct of Cph1 only fluoresces in the P_r form and with low quantum yield (*11*, *12*). Autoassembly with PEB leads to a Cph1 adduct that does not photoconvert since PEB lacks the $C_{15}{=}C_{16}$ double bond between the C and D rings of the tetrapyrrole chain. Instead, PEB adducts have a very high fluorescence quantum yield (*16*, *17*).

It is generally believed that plant phytochromes occur as homo dimers and that the PAS and carboxy terminal domains are involved in the intersubunit interactions (*6*, *18*). The cyanobacterial phytochrome Cph1 from *Synechocystis* has a lower molecular weight than plant phytochrome (85 vs 124 kDa), consisting of the N-terminal sensor module and the C-terminal transmitter modules but lacking the ~300 residue PAS module (*6*). It is, however, likely that Cph1 also forms homodimers since intersubunit transphosphorylation occurs in the P_r form and to a smaller extent also in the P_{fr} form (*2*). Evidence from size-exclusion chromatography suggests that Cph1 indeed forms dimers (*7*, *19*, *20*). These results are however contradictory and inconclusive. Here, we introduce a very sensitive fluorescence assay to detect Cph1 association by fluorescence resonance energy transfer (FRET) (*21*, *22*). This method is well-established in monitoring protein association (*22*), can be used in aqueous solution under native conditions, and does not suffer from possible artifacts associated with chromatographic methods. In favorable cases, FRET has also been used to measure chromophore−chromophore distances. We use time-resolved fluorescence with ps-excitation to measure the intensity and anisotropy decay of the PEB adduct of Cph1. This is an exceptionally sensitive fluorophore with an extinction coefficient of 85400 M^{-1} cm^{-1} (*17*) and a quantum yield of 0.72 (*17*). As the acceptor we chose either PEB (homo transfer) or the natural chromophore PCB (hetero transfer). Since each Cph1 monomer has only one chromophore binding site, it has only one fluorescent donor (PEB) or acceptor (PCB or PEB, respectively). Energy transfer thus only occurs in Cph1 dimers.

In this paper, we use two different experimental strategies to detect intersubunit energy transfer in the Cph1 dimer. In the first approach evidence for homo energy transfer was obtained with PEB/PEB homodimers. In the second set of complementary experiments evidence for hetero energy transfer was gathered using mixed PEB/PCB heterodimers. In either case the time-resolved fluorescence intensity and anisotropy were measured with samples that were sequentially titrated with PEB alone or with PEB and PCB, respectively.

In the homo energy transfer experiments, apo Cph1 was titrated with increasing amounts of PEB. As the concentration of doubly occupied PEB/PEB dimers increased, the fluorescence lifetime was unaltered, but the anisotropy progressively decreased, the experimental hallmark of homo energy transfer (*23*−*26*). Energy transfer leads to depolarization if the transition dipole moments are not parallel in the two subunits. The angle between these two directions was determined from the amplitude of the contribution of the energy transfer to the depolarization (*23*). Using this information and the 2-fold symmetry of the dimer it was shown that the angular factor κ^2 ranges between narrow limits and never approaches zero. This allowed a precise estimate of the inter-chromophore distance from the measured rate of homo energy transfer k_{HT}. Currently, no structural information is available on Cph1, and only low resolution results for plant phytochrome (*27*, *28*).

In the hetero energy transfer experiments apo Cph1 was first titrated to low occupancy with PEB (to minimize the contribution from homo energy transfer) and then titrated to full occupancy with the acceptor PCB. As the concentration of mixed PEB/PCB dimers increased the anisotropy was unaffected, but the intensity decay became progressively faster. Moreover, the decrease in lifetime was larger for the acceptor in the P_r form as compared to the P_{fr}/P_r photoequilibrium. These results provide unequivocal evidence for hetero energy transfer. From the change in mean fluorescence lifetimes, the rate of hetero energy transfer was estimated and found to be of the same magnitude as the more accurate value obtained from the homo energy transfer experiments.

Direct evidence for the existence of a Cph1 monomer/dimer equilibrium was obtained from the increase in anisotropy when PEB/PEB homo dimers were diluted. Dilution will ultimately lead to dissociation. These experiments allowed a first estimate of the dissociation constant.

To investigate the role of the transmitter module in the dimerization, additional experiments were performed with the deletion mutant Cph1Δ2, which consists of the first 513 amino acids from the N-terminus. The chromophore module is included in this sequence, but the C-terminal histidine kinase transmitter module is absent.

MATERIALS AND METHODS

Cph1 Expression and Purification, Bilin Chromophores. Recombinant *Synechocystis* PCC 6803 Cph1 (85 kDa) as well as a 58-kDa truncated fragment Cph1Δ2, lacking the C-terminal histidine kinase domain, were expressed with C-terminal $(His)_6$ tags in *E. coli*, purified on Ni^{2+}-NTA (Qiagen) and autoassembled with PCB or PEB as described (*1*, *7*). PCB and PEB were extracted from *Spirulina geitlerie* and *Porphyridium cruentum*, respectively, and purified via HPLC as described (*19*). Bilin stock solutions were prepared in methanol, and concentrations of stock solutions were estimated spectroscopically (*19*).

Time-Resolved Fluorescence Intensity and Anisotropy. Time-resolved fluorescence was measured using a home-built single-photon counting apparatus with picosecond time resolution. The samples were excited at 569 nm by pulses from a mode-locked Ti-sapphire laser (Millenia Vs and

Tsunami, Spectra Physics) that synchronously pumped a KTP-Ring OPO (optical parametrical oscillator) with intracavity frequency doubling with a LBO crystal (OPO Basic, APE). The initial repetition rate of the Ti-sapphire laser of 82 MHz was reduced to 4 MHz by synchronized pulse selection (Pulse Select, APE) of the frequency-doubled OPO output. The pulse-width was 1.5−2.0 ps (fwhm). The plane of polarization was rotated by an achromatic Fresnel rhomb. To achieve proper counting statistics, the excitation light pulse was attenuated by neutral density filters, resulting in typical excitation energies in the nanowatt range. The plane of polarization was set by a Glan−Thompson polarizer, and the beam was expanded to 5 mm diameter by a disperging lens. The fluorescence was collected at right angles to the excitation beam. A scattering suspension (LUDOX, Grace) was used to measure the instrumental response function (IRF, typical width 60 ps) at the excitation wavelength. The PEB fluorescence emission passed through a band-pass filter consisting of a cut-on color glass filter (OG 590) and a cutoff color filter (SP 640 nm, Coherent), a collimating lens and a sheet polarizer (Pol. UV2, Linos) and was detected by a microchannel plate photomultiplier (R3809U, Hamamatsu). The intensities $I_{||}(t)$ and $I_{\perp}(t)$ were detected successively by orienting the sheet polarizer parallel and perpendicular with respect to the excitation polarizer. The G-factor was measured as described (*29*, *30*). A time window of about 20 ns was selected with a time resolution of 15−20 ps per channel.

The fluorescence intensity decay ($I_{||} + 2I_{\perp}$) and time-resolved anisotropy decay $r(t)$ defined by

$$r(t) = \frac{I_{||}(t) - I_{\perp}(t)}{I_{||}(t) + 2I_{\perp}(t)} \tag{1}$$

were analyzed with a software using a nonlinear least squares iterative convolution method based on the Levenberg−Marquardt algorithm (*29*). The time courses of the fluorescence intensity and anisotropy decays were fitted with sums of exponentials

$$I(t) = \sum_i \alpha_i e^{-t/\tau_i} \tag{2}$$

$$r(t) = \sum_i \beta_i e^{-t/\phi_i} \tag{3}$$

Samples that were assembled with PCB were switched between the P_r and the P_{fr}/P_r photoequilibrium using appropriate light sources. Cph1 could be converted almost completely to the P_r state by illuminating the sample with a 3 mW LED (Quantum Devices) at 735 nm for 20 s. The P_{fr}/P_r photoequilibrium was reached using a 1 mW laser pointer at 650 nm for 1 min. The spectral state of the PCB sample was controlled by recording the absorption spectra.

Statistical Analysis of the Occupancies of the Chromophore Binding Sites in the Cph1 Dimer. With two chromophore binding sites per dimer that may be empty (0) or occupied by PEB (D, donor) or PCB (A, acceptor), there are six possible species: (D, D), (D, 0), (D, A), (A, A), (A, 0), and (0, 0). Let the number of dimers be N, the number of bound PEB molecules n_D and the number of bound PCB molecules n_A. Define x_D and x_A as the fractions of binding sites occupied with D and A, respectively

$$x_D \equiv \frac{n_D}{2N} \tag{4}$$

$$x_A \equiv \frac{n_A}{2N} \tag{5}$$

Let $P(X,Y)$ be the probability that the two binding sites are occupied with X and Y. $P(X,Y)$ is then also the fraction of dimers with X and Y bound. Assuming that the binding of PEB and PCB is noncooperative, random, and of equal strength, the probabilities are given by

$$P(\mathrm{D,D}) = x_D^2,\ P(\mathrm{D,0}) = 2x_D(1 - x_D - x_A),\ P(\mathrm{D,A}) = 2x_D x_A \tag{6}$$

$$P(\mathrm{A,A}) = x_A^2,\ P(\mathrm{A,0}) = 2x_A(1 - x_D - x_A),\ P(\mathrm{0,0}) = (1 - x_D - x_A)^2 \tag{7}$$

These six probabilities add up to one. Since only the PEB fluorescence is measured, only the probabilities P(D,D), P(D,0), and P(D,A) come into play. Suppose there is hetero energy transfer from D to A as well as homo transfer from D to D. Homo energy transfer does not affect the lifetime τ_D, and hetero energy transfer leads to a shorter lifetime τ_{DA}. For the mean lifetime $\bar{\tau}$ we then have

$$\bar{\tau} = \frac{[2P(\mathrm{D,D}) + P(\mathrm{D,0})]\bar{\tau}_D + P(\mathrm{D,A})\bar{\tau}_{DA}}{[2P(\mathrm{D,D}) + P(\mathrm{D,0}) + P(\mathrm{D,A})]} = (1 - x_A)\bar{\tau}_D + x_A\bar{\tau}_{DA} \tag{8}$$

We substituted for the Ps from eq 6. $\bar{\tau}$ will thus be a linearly decreasing function of x_A, and $(\bar{\tau}_{DA} - \bar{\tau}_D)$ may be determined from the slope.

Analysis of the Anisotropy Decay Data in the Presence of Homo Energy Transfer. The effect of homo energy transfer on the anisotropy was recently treated (*23*). These authors proposed that for two identical donors (here: PEB) the anisotropy is given by

$$r_{DD}(t) = \frac{1}{2}(r_1(t) + r_2(t))p(t) + \frac{1}{2}(r_{12}(t) + r_{21}(t))(1 - p(t)) \tag{9}$$

where $r_1(t) = r_2(t)$ is the anisotropy in the absence of energy transfer, which we will call r_{D0}

$$r_{D0}(t) \equiv r_1(t) = (r_\circ - \beta)e^{-t/\phi_1} + \beta e^{-t/\phi_2} \tag{10}$$

In eq 10, r_o is the initial anisotropy, ϕ_1 is the rotational correlation time of the chromophore in its binding pocket, and ϕ_2 represents the rotation of the whole dimer. $p(t)$ is the excitation probability, with k_{HT} the rate constant for homo energy transfer

$$p(t) = \frac{1}{2}(1 + f(k_{HT}t)) \tag{11}$$

$$k_{HT} = \frac{1}{\tau_D}\left(\frac{R_o}{R_{DD}}\right)^6 \tag{12}$$

$f(k_{HT}t)$ is usually a single exponential (*23*) or a powerlaw (*31*)

$$f(k_{HT}t) = e^{-2k_{HT}t} \quad (13)$$

$$f(k_{HT}t) = \left(1 + \frac{2k_{HT}t}{n}\right)^{-n} \quad (14)$$

Eq 14 reduces to eq 13 in the limit $n \rightarrow \infty$. Powerlaws are more appropriate in the presence of structural or spectral heterogeneity, which leads to a distribution of rates.

R_o is the Förster distance for homo energy transfer, and R_{DD} is the donor−donor distance. r_{12} and r_{21} are the transfer anisotropies given by (*23*)

$$r_{12} = r_{21} = P_2(\cos\delta) r_{D0}(t) \quad (15)$$

Here, P_2 is the second Legendre polynomial, and δ is the angle between the two transition dipole moments. Substituting eqs 10, 11, and 15 in eq 9, we obtain

$$r_{DD}(t) = \left[\left(\frac{1 + P_2(\cos\delta)}{2}\right) + \left(\frac{1 - P_2(\cos\delta)}{2}\right) f(k_{HT}t)\right] r_{D0}(t) \quad (16)$$

Eq 16 shows that r_{DD} can be factorized in r_{D0}, which describes the depolarization in the absence of energy transfer and the first factor that contains the information on the rate k_{HT} and on the angular change δ of the transition dipole moment. In the absence of energy transfer, $k_{HT} \rightarrow 0$, $f \rightarrow 1$, and r_{DD} reduces to r_{D0}. The amplitude of the second time-dependent term in the first factor, the contribution from homo energy transfer, is proportional to $(1 - P_2)$. When the two transition dipoles are parallel, this factor is zero, as it should be. The transfer of excitation to a transition dipole with the same orientation does not lead to depolarization. From eq 16 we see that measurement of $r_{DD}(t)$ not only allows us to determine the rate of energy transfer (k_{HT}) but also provides information on the structural parameter δ. δ in turn enters the orientational factor κ^2, which plays an important role in the interpretation of k_{HT} in terms of the donor−donor distance.

When not all of the chromophore binding sites are filled, we have a mixture of dimers with two, one, or zero chromophores. Only those with at least one chromophore will fluoresce. Using eq 1, we can calculate the observed anisotropy $r(t)$ of the mixture

$$r(t) = \frac{P(D,0) r_{D0}(t) S_{D0}(t) + 2P(D,D) r_{DD}(t) S_{DD}(t)}{P(D,0) S_{D0}(t) + 2P(D,D) S_{DD}(t)} \quad (17)$$

$S(t)$ is the total fluorescence intensity $I_{\parallel}(t) + 2I_{\perp}(t)$. Since homo transfer does not affect the decay curve (*26*), $S_{D0} = S_{DD}$, and the S factors drop out. Substituting for $P(D,0)$ and $P(D,D)$ from eq 6, we obtain the simple expression

$$r(t) = (1 - x_D) r_{D0}(t) + x_D r_{DD}(t) \quad (18)$$

$r(t)$ is thus a linear superposition of the anisotropies r_{DD} and r_{D0} with weights $(1 - x_D)$ and x_D, respectively. For experiments (labeled by i) with different fractions $x_i \equiv x_{D,i}$ of the binding sites occupied we have

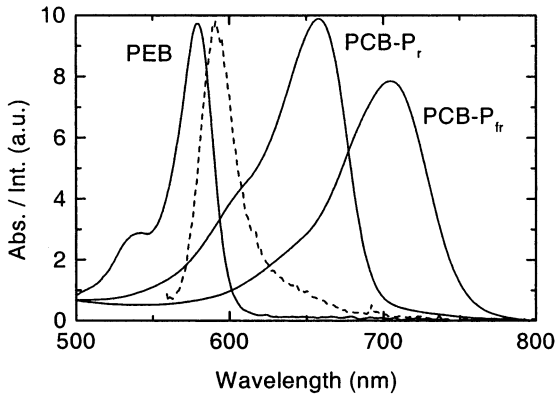

FIGURE 1: Absorption spectra of PCB and PEB bound to Cph1 (—) and the emission spectrum of PEB bound to Cph1 (- - -). The absorption spectrum of PCB depends on whether phytochrome is in the P_r or P_{fr} form. The spectral overlap between PEB emission and PCB absorption is clearly larger in the P_r state.

$$r_i(t) = (1 - x_i) r_{D0}(t) + x_i r_{DD}(t) \quad (19)$$

With more than two values of x_i, eq 19 is an overdetermined system of linear equations for the time traces $r_{D0}(t)$ and $r_{DD}(t)$. We may write eq 19 in matrix form as

$$\boldsymbol{r} = \boldsymbol{M}\boldsymbol{R} \quad (20)$$

with $R_{1t} = r_{D0}(t)$, $R_{2t} = r_{DD}(t)$, and $\boldsymbol{M}$ the x_i-containing coefficient matrix. The pure r_{D0} and r_{DD} traces may now be calculated using the pseudo-inverse $\boldsymbol{M}^{-1}$ in eq 20

$$\boldsymbol{R} = \boldsymbol{M}^{-1}\boldsymbol{r} \quad (21)$$

Fitting $r_{D0}(t)$ to eq 10 and r_{DD}/r_{D0} to eq 16 with exponentials or powerlaws then allows us to determine the rotational correlation times and the homo energy transfer parameters (k_{HT}, n, and δ). Using eq 19 fit curves, r_i can be constructed for each x_i and may be compared with the data r_i.

RESULTS

Hetero Energy Transfer in Mixed PEB/PCB Dimers. Let us first estimate whether the range of energy transfer for the donor/acceptor pairs PEB/PEB and PEB/PCB as measured by the Förster radius R_o is large enough to make energy transfer between the subunits of Cph1 likely. The absorption and emission spectra of Cph1 regenerated with PEB and PCB are shown in Figure 1. The spectrum of the pure P_{fr} state was constructed from the measured spectra of P_r and the P_{fr}/P_r photoequilibrium, in good agreement with the P_{fr} spectrum published in ref *7*. From these data and the extinction coefficients at the absorption maxima of PEB (*17*) and PCB (*19*) bound to Cph1, the spectral overlap integrals J were calculated by numerical integration. In this way, we found $J = 3.6 \times 10^{-13}$ cm^3 M^{-1} for the donor−acceptor pair PEB/PEB, $J = 4.1 \times 10^{-13}$ cm^3 M^{-1} for the pair PEB/PCB_{Pr}, and $J = 1.6 \times 10^{-13}$ cm^3 M^{-1} for the pair PEB/PCB_{Pfr}. The reduced value in the P_{fr} state is due to the red shift of the P_{fr} absorption spectrum with respect to that of P_r and its smaller extinction coefficient (see Figure 1). These results indicate that if the transition dipole moment orientations are approximately the same in the PEB/PEB and PEB/

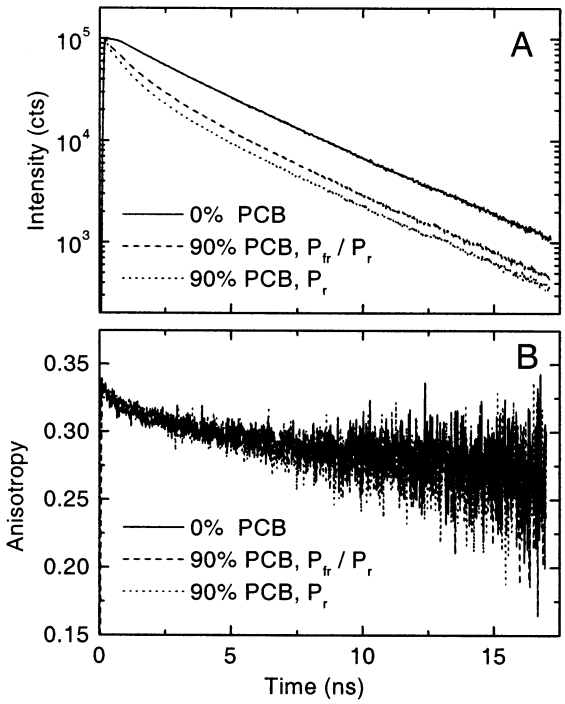

FIGURE 2: Hetero energy transfer in mixed PEB/PCB Cph1 dimers. Apo Cph1 was assembled at low PEB concentration ($x_D = 0.1$) and then titrated with PCB from $x_A = 0.06$ to $x_A = 0.90$. Measurements were performed at $x_A = 0.0$, 0.06, 0.32, 0.56, and 0.90 both in P_r and in P_{fr}/P_r photoequilibrium. For clarity, only the time traces at $x_A = 0.0$ and 0.90 are shown. Conditions: Cph1 monomer concentration 8.4 μM, pH 7.8, 50 mM Tris, 5 mM EDTA, 15 °C. (A) Intensity decay. (B) Anisotropy decay.

PCB dimers, the rates for energy transfer should also be about the same. Since the chromophores are expected to be tightly bound in their binding pockets (born out by the high anisotropy values for PEB, see Figure 2B below), we have no a priori knowledge about the orientational factor κ^2. When we make the assumption $\kappa^2 = {}^2/_3$, $\phi_{PEB} = 0.72$ (*17*), and $n^4 = 4$, we obtain for the Förster radii values of 58.0, 59.3, and 50.7 Å for PEB/PEB, PEB/PCB_{Pr} and PEB/PCB_{Pfr}, respectively. This calculation shows that R_o is quite large. In view of the estimates of 70−150 Å for the chromophore−chromophore distance in plant phytochrome from low resolution structural methods (*27*, *28*), we conclude that both homo and hetero energy transfer may well occur in Cph1 dimers unless κ^2 is close to zero. Since we can exclude this possibility (see eq 22 and Figure 6 below), we expect to observe energy transfer.

To investigate hetero energy transfer from PEB to PCB in the absence of PEB/PEB homo transfer, apo Cph1 was first assembled with 10% PEB (as determined from the absorption spectrum). At this low level of occupancy ($x_D = 0.1$) and assuming noncooperative binding, the fraction of Cph1 dimers with both binding sites occupied by PEB is expected to be rather small ($(0.1)^2$, see eq 6). The contribution from PEB/PEB homo transfer, which does not affect the lifetime, is therefore small. This sample was then further titrated with PCB. The fluorescence intensity decay was measured at PCB percentages that varied from 0 to 90%. In terms of x_A of eq 5, x_A was varied from 0.0 to 0.9. With increasing PCB percentage, the number of mixed PEB/PCB dimers increased linearly ($P(D,A) = 2x_D x_A$, eq 6). In the final state (10% PEB/90% PCB) all the binding sites were

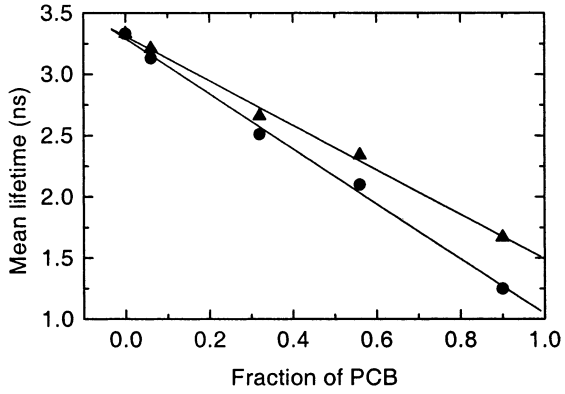

FIGURE 3: Mean lifetime $\bar{\tau}$ of PEB ($x_D = 0.1$) as a function of x_A, the fraction of binding sites occupied with PCB. $\bar{\tau}$ was calculated from the data in Figure 2A. ●: P_r (illumination at 735 nm); ▲: P_{fr}/P_r photoequilibrium (illumination at 650 nm).

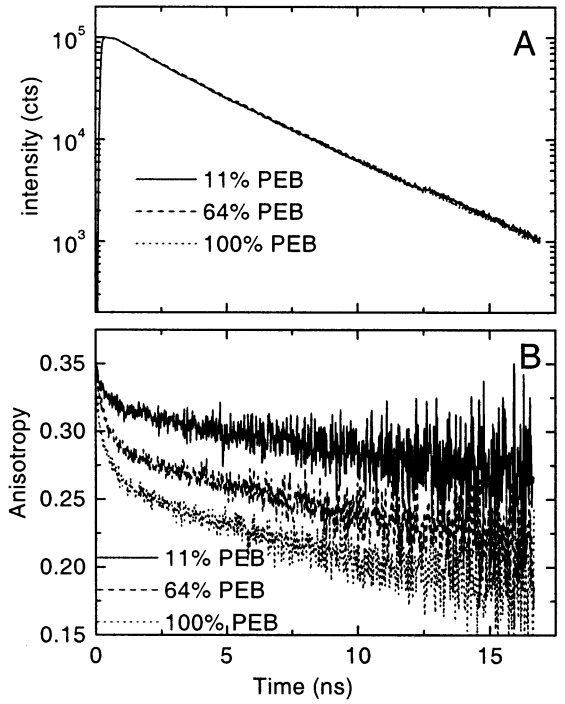

FIGURE 4: Homo energy transfer in PEB/PEB Cph1 dimers. Apo Cph1 was assembled with PEB. x_D, the fraction of binding sites occupied with PEB was varied between 0.10 and 1.00. Measurements were performed at $x_D = 0.11$, 0.20, 0.41, 0.64, and 1.00. For clarity, only the traces at $x_D = 0.11$, 0.64, and 1.00 are shown. Conditions: Cph1 monomer concentration 10.6 μM, pH 7.8, 50 mM Tris, 5 mM EDTA, 15 °C. (A) Intensity decay. (B) Anisotropy decay.

filled, and most of the bound PEB was in mixed PEB/PCB dimers. With increasing PCB, the PEB fluorescence intensity decay became faster. Figure 2A shows the data for 0% PCB and the end value of 90% PCB. Using far-red or red illumination, the PCB monomers were converted between the P_r state and the photoequilibrium of the P_r and P_{fr} states (about 65% P_{fr}). At every percentage PCB, the decay in the P_r state was faster than in the P_r/P_{fr} mixture obtained by red light illumination. This effect is shown for 90% PCB in Figure 2A (for clarity the decay curves at 6, 32, and 56% PCB in P_r and P_{fr} are not shown, their time courses being intermediate). Even at 10% PEB in the absence of acceptor the decay was not monoexponential but biexponential with $\bar{\tau} = 3.33$ ns. At 90% PCB, four exponentials were required

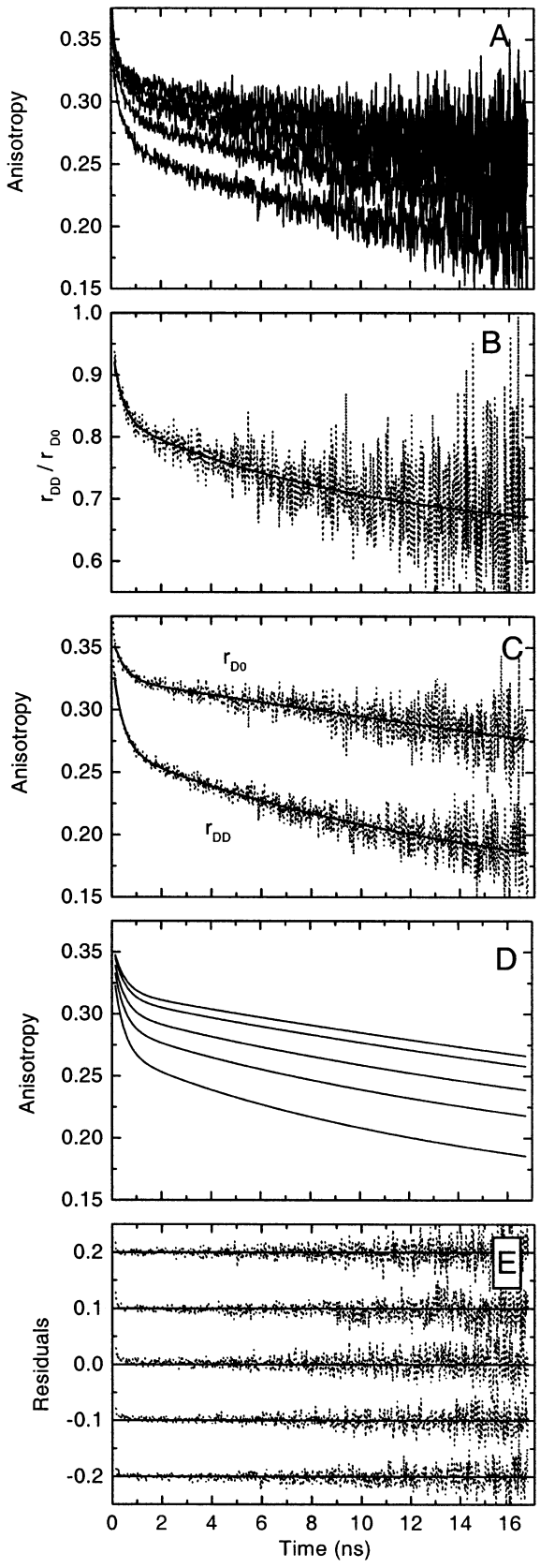

FIGURE 5: Global analysis of the anisotropy data of Figure 4B. (A) Expanded anisotropy data with from top to bottom $x_D = 0.11$, 0.20, 0.41, 0.64, and 1.00. (B) The ratio r_{DD}/r_{D0} obtained from eq 21 and its fit to eq 16. (C) Fit of r_{D0} to eq 10 and of r_{DD} according to eq 16. (D) Fits of the five $r_i(t)$-traces in panel A according to eq 19 using the fitted r_{D0} and r_{DD} traces and the experimental x_i values. (E) Residuals between the five data sets (A) and the corresponding fit curves (D). The five sets of residuals are offset by 0.1.

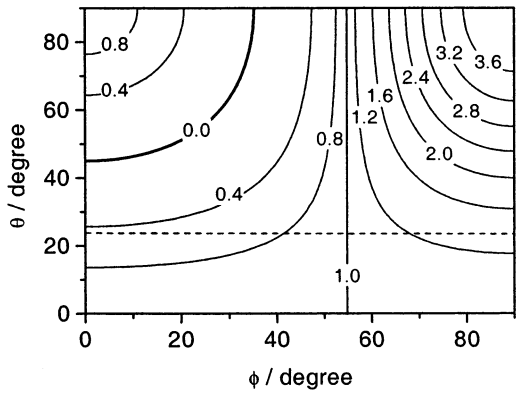

FIGURE 6: Contour plot of κ^2 (θ,ϕ) for the chromophores of the Cph1 PEB homo dimer according to eq 22. θ and ϕ are the spherical polar coordinates of one chromophore in its local coordinate system defined in the text. $\kappa^2 = 4$ at the upper right corner and 1 at the other three corners. $\kappa^2 = 0$ along the curve in the upper left corner. From the amplitude of the contribution of homo transfer to the anisotropy, θ was found to be 22.5°. The dashed horizontal line at $\theta = 22.5°$ shows that κ^2 increases from a minimum of 0.500 at $\phi = 0°$ to a maximal value of 1.313 at $\phi = 90°$.

for a good fit. Under these conditions $\bar{\tau}$ was 1.25 ns for P_r and 1.67 for the P_r/P_{fr} mixture. In Figure 3 $\bar{\tau}$ is plotted versus the fraction PCB (x_A). $\bar{\tau}$ decreases linearly with PCB both for P_r (●) and the P_{fr}/P_r photoequilibrium (▲). This linear dependence is expected if, due to energy transfer, the lifetime of PEB is shorter in the mixed PEB/PCB hetero dimer than in the PEB/empty dimer (see eq 8). From the slopes of the fit curves of Figure 3 we obtained values of $\bar{\tau}_{DA} = 1.02$ ns for P_r and $\bar{\tau}_{DA} = 1.49$ ns for the P_{fr}/P_r photoequilibrium. We can obtain a rough estimate of the efficiency of energy transfer from $E = 1 - \bar{\tau}_{DA}/\bar{\tau}_D$ using the mean lifetime of the donor alone (3.33 ns) and of the donor in the presence of the acceptor (1.02 ns in the P_r state and 1.49 in the P_r/P_{fr} photoequilibrium). In this way, we obtain $E = 0.69$ in P_r and $E = 0.55$ in the P_r/P_{fr} mixture. Since the photostationary mixture consists of approximately 65% P_{fr} and 35% P_r, the actual difference in energy transfer efficiency between the pure P_r and the P_{fr} states is substantially larger than these numbers suggest. The stronger energy transfer in P_r could be explained by the larger spectral overlap if we assume that κ^2 is the same. This assumption is however weak since due to the isomerization of PCB the orientation of the acceptor transition dipole moment will differ in P_r and P_{fr}. Using the difference in the mean lifetimes we could calculate a rate of energy transfer and from this estimate the donor−acceptor distance. Such an analysis is questionable however on two counts: the use of the mean lifetime and the lack of information about κ^2.

The anisotropy $r(t)$ did not vary with the percentage PCB. The traces for 0 and 90% PCB are shown in Figure 2B. With $r(0) = 0.34$ the initial anisotropy is quite high. An initial rapid phase ($\phi_1 \sim 0.8$ ns) of small amplitude is followed by a very slow decay with $\phi_2 \sim 95$ ns, which is presumably due to the slow rotation of the whole Cph1 dimer. For PEB/PCB hetero energy transfer the PEB anisotropy is not expected to depend on the amount of energy transfer.

Homo Energy Transfer in PEB/PEB Dimers. In these experiments, apo Cph1 was titrated with PEB, and at each concentration $I(t)$ and $r(t)$ were measured. At low percentage regeneration only one of the two binding pockets of the dimer

is occupied with PEB. At higher percentages of regeneration the fraction of dimers with both binding sites occupied with PEB starts to increase (P(D,D) = x_D^2) and with it the occurrence of PEB/PEB homo energy transfer. The hallmark of homo energy transfer is that the lifetime is unaffected but that, unless the two transition dipoles are parallel, additional depolarization occurs. This is exactly what was observed. The intensity traces in Figure 4A show that the decay remains the same with increasing regeneration. Of the measurements at 11, 20, 41, 64, and 100% PEB, only three traces are shown. All $I(t)$ traces coincided and had a $\bar{\tau}$ of 3.22 ns, close to that for the case of no PCB in Figure 2A. As is apparent from Figure 4B, large effects were observed in the anisotropy decay with a significant and systematic decrease in anisotropy with increasing concentration of PEB/PEB dimers. For clarity the traces at 20 and 41% PEB, which lie between the traces at 11, 64, and 100% PEB, are not shown. At low percentage regeneration (x_D = 0.1), the fraction of double occupied dimers P(D,D) is $(0.1)^2$ and thus quite low. The observed fluorescence, however, is due to those dimers with bound PEB. The fraction of doubly occupied dimers is about 10%; thus, their contribution cannot be neglected. The trace in Figure 4B at x_D = 0.1 therefore still contains a substantial contribution from homo energy transfer and cannot be identified with the state (D,0). To extrapolate to the $r(t)$ traces for the two states with no homo energy transfer r_{D0} and with complete energy transfer r_{DD}, we use the scheme described in eqs 16−21 of Materials and Methods. Each of the $r(t)$ traces at the five x_D values can be written as a linear superposition according to eq 19. The overdetermined system of linear equations for r_{DD} and r_{D0} can be solved according to eq 21. The resulting time traces for the ratio r_{DD}/r_{D0} and r_{DD}, r_{D0} are shown in panels B and C of Figure 5 together with their fits according to eqs 10 and 16. r_{D0} describes the rotational dynamics of chromophore and phytochrome in the absence of homo energy transfer. The fit parameters were ϕ_1 = 0.47 ns and ϕ_2 = 105 ns. These numbers are in good agreement with those obtained from the hetero energy transfer data of Figure 2B. The chromophore thus executes a rapid wobbling motion of small amplitude within the binding pocket (ϕ_1). ϕ_2 is due to the slow tumbling of the dimer. The fit of r_{DD}/r_{D0} to eq 16 was also satisfactory (see Figure 5B). The powerlaw fit led to the fit parameters $P_2(\cos\delta)$ = 0.2445, $(k_{HT})^{-1}$ = 2.15 ns, and n = 0.34. Multiplying the fit-curve for r_{D0} by the fit-curve for r_{DD}/r_{D0}, we also have the fit for r_{DD}. Using these fits for r_{DD} and r_{D0}, the corresponding fits for the $r_i(t)$ traces were constructed using the values of x_i in eq 19. These fits are shown in Figure 5D and should be compared with corresponding experimental time traces in Figure 5A. Because of the large number of closely spaced and noisy curves, we refrained from superimposing the data and the fits in one panel. Instead, we show the residuals in Figure 5E. These indicate that a satisfactory fit was achieved with the three above parameters. With $P_2(\cos\delta)$ = 0.245, we find $\delta = 45 \pm 5°$.

Chromophore−Chromophore Distance in PEB/PEB Dimers. Distance calculations based on energy transfer are often associated with large errors due to uncertainty about the angular factor κ^2 (*21*, *22*). This is in particular so in cases such as the phytochrome dimers considered here where the chromophore transition dipole moments are expected to have well-defined fixed but unknown orientations. Taking the orientational average of κ^2 is certainly unjustified. κ^2 depends on the cosines of three angles: between the two transition dipole moment directions and between each of the transition dipole moments and the vector connecting the two chromophores. Above, we determined the first angle from the amplitude of the depolarization due to homo transfer. This puts a great constraint on the possible values of κ^2. A further constraint is due to the fact that in the homo transfer we are dealing with identical PEB chromophores that are excited and emit in the same S_o transition. The absorption and emission dipoles are thus identical leading to the high $r(0)$ value of 0.34−0.36 observed. Let (θ,ϕ) be the spherical polar coordinates of one transition dipole moment in a rectangular coordinate system (x,y,z) that is fixed with its origin at this chromophore position and oriented with respect to the vector connecting the two chromophores in such a way that y is parallel to the connecting vector, and z is parallel to the 2-fold symmetry axis of the dimer (perpendicular to the connecting vector). Because of the 2-fold symmetry, the spherical polar coordinates of the other transition dipole moment are then $(\theta,\phi + \pi)$. The expression for κ^2 now only depends on θ and ϕ and takes the simple form

$$\kappa^2(\theta,\phi) = [\cos 2\theta + 3\sin^2\theta\sin^2\phi]^2 = [1 + \sin^2\theta\{3\sin^2\phi - 2\}]^2 \quad (22)$$

A contour plot of κ^2 is shown in Figure 6. Of particular interest is the curve defined by $\kappa^2 = 0$. As long as we are sufficiently far away from this valley, the error in R_{DA} will be small since R_{DA} is proportional to the sixth root of κ^2. Since we actually determined the angle $\delta = 2\theta$ between the two transition dipole moments to be $45 \pm 5°$, $\theta = 22.5 \pm 2.5°$. Without further knowledge about the value of ϕ, we now have according to eq 22

$$\kappa^2(22.5°,\phi) = [0.707 + 0.439\sin^2\phi]^2$$

Thus, κ^2 increases monotonically along the horizontal line at $\theta = 22.5°$ (dashed line in Figure 6) from the minimum of 0.500 at $\phi = 0$ to the maximal value of 1.313 at $\phi = \pi/2$ and is always well-removed from 0. Taking the sixth root, we find 0.89 at $\phi = 0$ and 1.05 at $\phi = \pi/2$. Thus, R_{DA} is at most 5% larger or 11% smaller than the value calculated with $\kappa^2 = 1$.

To calculate R_{DA}, we need the rate k_{HT} of homo energy transfer that we determined from the fit to the data of Figure 5A. The result was $(k_{HT})^{-1}$ = 2.15 ns. Using $J = 3.6 \times 10^{-13}$ cm^3 M^{-1}, $n^4 = 4$, ϕ_{PEB} = 0.72, κ^2 = 2/3, and $\bar{\tau}$ = 3.33 ns in eq 12, we find R_{DA} = 53.8 Å. Using the bounds on κ^2 derived above R_{DA} is resticted to the range 51.2 Å < R_{DA} < 60.4 Å. This estimate only takes into account the uncertainty in κ^2 and does not include the experimental errors in θ, k_{HT}, J, and $\bar{\tau}$. The error in θ is the most important source of error since it determines how close κ^2 can get to zero. From eq 22 and Figure 6, we note that κ^2 can only become zero when $\theta \geq 45°$. Taking all error sources into account we arrive at the range 49 Å < R_{DA} < 63 Å.

Dimer Dissociation by Dilution. Fully reconstituted PEB/PEB dimers were diluted with buffer. If the dimers do not dissociate upon dilution, $I(t)$ and $r(t)$ should be unaffected. If, however, the dimerization equilibrium is shifted to the

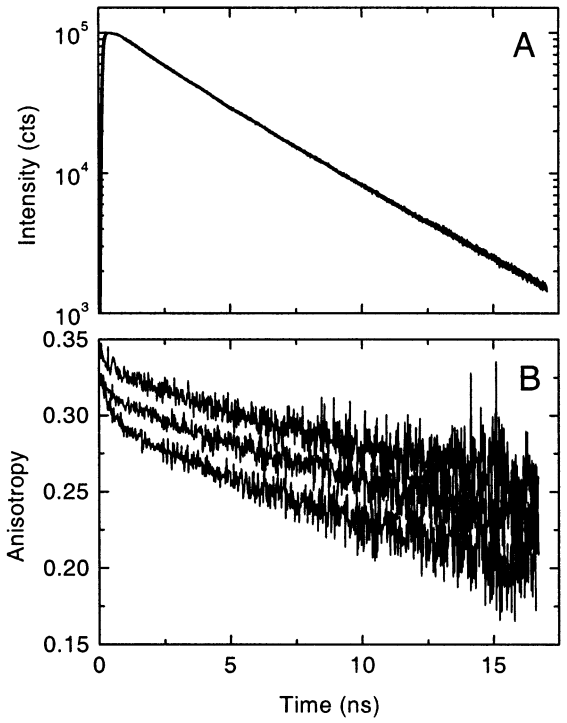

FIGURE 7: Effect of dilution-induced dimer dissociation on homo energy transfer. Cph1 was completely regenerated with PEB and then diluted from 11 to 0.19 μM. Conditions: pH 7.8, 50 mM Tris, 5 mM EDTA, 15 °C. (A) Intensity decays at the seven concentrations 11, 6.7, 3.9, 2.0, 1.1, 0.49, and 0.19 μM. B. Anisotropy decays. From bottom to top the traces are at the concentrations 11, 3.9, and 0.19 μM.

side of PEB monomers, there will be less homo transfer. This should be reflected in unaltered $I(t)$ traces and a progressive increase in the anisotropy with decreasing concentration of dimers. The concentration of PEB monomers was varied approximately 50-fold between 11 and 0.19 μM. $I(t)$ and $r(t)$ were measured at the seven concentrations 11, 6.7, 3.9, 2.0, 1.1, 0.49, and 0.19 μM. Figure 7A shows that the lifetime is virtually unaffected, with the mean lifetime varying between 3.34 and 3.53 ns. The anisotropy (Figure 7B) on the other hand is clearly affected by the dilution. With decreasing concentration the anisotropy increases, as expected for decreasing homo energy transfer. For clarity, only the traces at 11, 3.9, and 0.19 μM are shown in Figure 7B. At the lower concentrations, the experimental effect of an increase in $r(t)$ saturated, suggesting that at these concentrations the dissociation is complete. From these data, we estimated the dissociation constant K_D in the following way. The concentration dependence of the effect in the anisotropy was plotted, and the K_D was set equal to the concentration at which the effect was half saturated. In this way, we obtained the rough estimate $K_D = 5 \pm 3$ μM. We note that the trace at 3.9 μM is about halfway between the traces at 11 μM (mostly dimers) and 0.19 μM (mostly monomers). For a quantitative evaluation more accurate data over a wider concentration range are required and a more elaborate data analysis based on the dimerization model. We note that the slowest rotational correlation time in the trace at 0.19 μM in Figure 7B is 62 ns and therefore represents the overall tumbling time of the Cph1 monomer.

Deletion Mutant Cph1Δ2. This mutant protein consists of the first 513 amino acids from the N-terminus. It contains

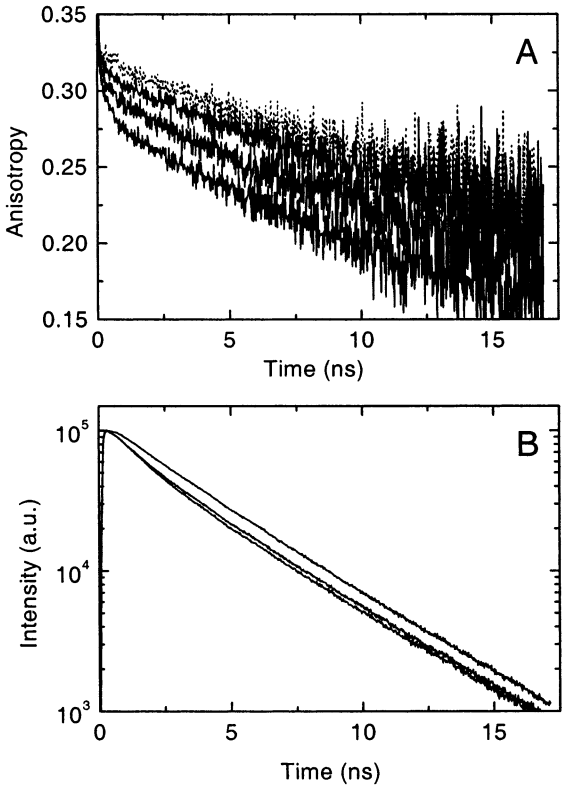

FIGURE 8: Energy transfer in the deletion mutant Cph1Δ2. (A) Anisotropy decay $r(t)$. Conditions: pH 7.8, 50 mM Tris, 5 mM EDTA, 15 °C. The molar PEB/Cph1Δ2 ratios and Cph1Δ2 concentrations are from top to bottom traces: 1.0 and 0.25 μM; 0.12 and 12.5 μM; 0.53 and 12.5 μM; and 1.0 and 12.5 μM. B. Intensity decay $I(t)$. Conditions: 12.5 μM Cph1Δ2, pH 7.8, 50 mM Tris, 5 mM EDTA, 15 °C. The molar PEB/Cph1Δ2 and PCB/Cph1Δ2 ratios for the three traces are from top to bottom: 0.13 and 0.0; 0.13 and 0.72 in P_r; and 0.13 and 0.72 in P_r/P_{fr} photoequilibrium.

the chromophore-bearing sensory module and has absorption spectra and photocycle kinetics (*9*) similar to those of the full-length protein. It lacks the transmitter module, comprising the kinase domain, the H538 phosphoacceptor subdomain, and the response-regulator-binding domain. The transmitter module is thought to be largely responsible for the dimerization necessary for the mutual transphosphorylation seen in the sensory histidine kinase family.

Apo Cph1Δ2 was regenerated with PEB at molar chromophore/monomer ratios of 0.12, 0.53, and 1.00 (determined spectroscopically) at a protein concentration of 12.5 μM. The PEB intensity decay was virtually unaffected, and the mean lifetime varied between 3.11 and 3.25 ns in these three samples. The anisotropy decay showed qualitatively the same effect as with full-length Cph1 (Figure 4B). As shown in Figure 8A the anisotropy clearly decreased with increasing PEB binding, suggesting some homo energy transfer. Dilution from 12.5 to 0.25 μM at a 1.0 ratio PEB/Cph1Δ2 led moreover to complete abolishment of this depolarization effect (Figure 8A, top trace), suggesting dissociation of dimers with concomitant loss of energy transfer. Under these conditions, the deletion mutant is thus predominantly in the monomeric state. The measured rotational correlation time was 50 ns, which is thus that of a Cph1Δ2 monomer (MW 58 kDa).

Further support for dimerization of the deletion mutant was obtained from the corresponding hetero energy transfer

experiments. After reconstitution with low amount of PEB (PEB/Cph1Δ2 = 0.13) to avoid homo transfer, a large amount of PCB was added (PCB/Cph1Δ2 = 0.72). This had no effect on the anisotropy (data not shown) but had a significant effect on the intensity decay (Figure 8B). The mean lifetime decreased from 3.38 ns with 0.13 PEB and 0.0 PCB to 2.85 ns with 0.13 PEB and 0.72 PCB in the P_r state. In the photostationary P_r/P_{fr} mixture (65% P_{fr}), the mean lifetime decreased further to 2.67 ns. In the deletion mutant, hetero energy transfer is thus stronger in P_{fr} than in P_r, in contrast to full-length Cph1, where the opposite effect was observed. Repeated switching between the P_r and the P_{fr} states showed that this difference in $\bar{\tau}$ was reproducible. These results clearly suggest hetero energy transfer in mixed PEB/PCB dimers, in agreement with the conclusions from homo transfer. These experiments were performed at a protein concentration of 12.5 μM. Experiments with the full-length protein were performed at the lower concentration of 8.4 μM and led to much larger decreases in $\bar{\tau}$ (Figure 2A): from 3.33 ns to 1.25 and 1.67 ns in P_r and P_r/P_{fr}, respectively. Comparing the results of homo transfer between the deletion mutant Cph1Δ2 (Figure 8A) and full-length Cph1 (Figure 4B), we also conclude that the effect is smaller in Cph1Δ2. Removal of the C-terminal domain in Cph1Δ2 thus probably leads to a reduction in dimerization.

DISCUSSION

The dimerization of phytochrome is of considerable biological significance. In Cph1 it allows for the efficient intersubunit trans-phosphorylation that differs in P_r and P_{fr} and is regulated by light. Moreover, dimerization modulates the kinetics of dark reversion from P_{fr} to P_r (*32*) and most likely also affects the interaction with the response regulator. It is thus useful to have available a fluorescence assay to monitor the dimerization with high sensitivity. In this paper, we showed that homo and hetero energy transfer between the chromophores of each dimer subunit of Cph1 provide such an assay. We could interpret the homo energy transfer data in terms of the distance and the angle between the chromophore transition dipole moments. The hetero energy transfer data indicated that the rate of energy transfer is larger in P_r than in P_{fr}. This may be due to the closer proximity of the chromophores in P_r and may be related to the higher histidine kinase activity in P_r. We found, moreover, that the loss of homo energy transfer upon dilution is due to dimer dissociation allowing an estimate for the K_D.

The data of Figure 4 indicated that with increasing concentration of PEB/PEB dimers the PEB lifetime was unaffected (Figure 4A), but the depolarization increased (Figure 4B). This is the experimental signature of homo energy transfer. The anisotropy data were then analyzed using eq 16, which shows that the anisotropy r_{D0} in the absence of energy transfer is multiplied by a factor that contains the time dependence of the homo transfer ($f(k_{HT}t)$) and the angle δ between the two transition dipole moments. As shown in Figure 5, the anisotropy data at five different PEB to Cph1 ratios could be fitted simultaneously in this way leading to the common fit parameters $k_{HT}^{-1} = 2.51$ ns and $\delta = 45 \pm 5°$. Using this value of δ and an analytic expression for κ^2 based on the 2-fold chromophore symmetry in the dimer, we could show that the allowed κ^2 values are in a narrow range (Figure 6). This constraint on κ^2 allowed us to derive a correspondingly narrow range of 49 Å < R_{DA} < 63 Å for the PEB−PEB distance from the measured rate of energy transfer.

Figure 2 shows that when Cph1 dimers that were first reconstituted with 10% PEB are further titrated with the acceptor PCB, the lifetime becomes faster (Figure 2A), but the anisotropy decay is unaffected (Figure 2B). This is the hallmark of hetero energy transfer. These experiments were performed in the pure P_r form as well as in the P_{fr}/P_r photoequilibrium (~65% P_{fr}). Figure 3 shows that the mean lifetimes in these two states decrease linearly with increasing fraction of binding sites that are occupied by the acceptor PCB. This is in accordance with eq 8 for hetero energy transfer and allowed us to determine mean lifetimes of 1.02 and 1.49 ns for the PEB/PCB hetero dimers in P_r and the P_{fr}/P_r photoequilibrium, respectively.

The dilution assay provided direct evidence for dimerization but required the use of time-resolved fluorescence depolarization equipment. The question arises whether these effects could not also be observed with steady-state fluorescence depolarization methods that are more readily available and would allow routine tests of the effect of mutations on phytochrome dimerization. Rather than measure the steady-state anisotropy values $\langle r \rangle$, we calculated them from the measured time-dependence of $r(t)$ and $I(t)$. This is a routine and reliable procedure for which we used the fit parameters α_i, β_i, ϕ_i, and τ_i of eqs 2 and 3. In this way, we found that in the dilution experiments of Figure 7B the corresponding steady-state anisotropy values $\langle r \rangle$ increased from 0.27 at 11 μM to 0.31 at 0.19 μM. The reason that the effect in $\langle r \rangle$ is less than in $r(t)$ is due to the weighting of $r(t)$ by $I(t)$. In this way, the small lifetime of bound PEB reduces the effect. At present it seems therefore that the steady-state effect is probably too small since the absolute values of $\langle r \rangle$ in different samples of wild type and mutants need to be compared.

Only low resolution structural information is available for pea photochrome (*27*, *28*). These data led to a quaternary structure model with a 2-fold symmetry axis, with the C-terminal domains involved in subunit interactions and the N-terminal chromophore domains separated by distances ranging from 70 (*27*) to 150 Å (*28*). Cph1 is a histidine kinase. Currently available high-resolution structures of other histidine kinases (reviewed in refs *33* and *34*) indeed display 2-fold symmetry. Here we have used homo energy transfer to find an interchromophore distance of about 56 ± 7 Å. Homo energy transfer manifests itself through increased depolarization but only if the angle between the transition dipole moments differs from zero. The amplitude of homo energy transfer is proportional to $(1 - P_2(\cos 2\theta))$, where 2θ is this angle (eq 16). The maximal effect thus occurs as expected when the angle is 90°. The amplitude therefore contains important structural information on the transition dipole moment geometry that is required in the calculation of the inter-chromophore distance from the transfer rate k_{HT}. Our experiments thus demonstrate that homo energy transfer supplies crucial additional structural information on the angle between the chromophore transition dipole moments that is not available from hetero energy transfer experiments. In the latter, the only available information is the change in the mean lifetime. It is difficult to interpret the homo energy transfer efficiency, which may be calculated from the mean

lifetimes, since four components contribute to $\bar{\tau}$ in the presence of energy transfer. A proper analysis of hetero energy transfer in case of multiple lifetimes is currently not available. Homo energy transfer thus seems to be the method of choice. An essential prerequisite for the application of homo energy transfer through its effect on the anisotropy is that the fluorophores are immobilized. This ensures that the anisotropy remains high and does not decay due to rapid large angle rotational diffusion. This condition was met in the present case with the PEB chromophores immobilized in the binding pocket and with only a small amplitude rapid wobbling motion (see Figures 2B and 4B).

As discussed, an analysis of hetero energy transfer in the presence of multiple lifetimes, in the absence of a priori information on κ^2, with immobilized donor and acceptor and in the absence of 2-fold symmetry is difficult. We may nevertheless use the mean lifetimes of PEB in the absence and presence of the PCB acceptor, to obtain a rough estimate of the rate of hetero energy transfer. For the P_r state, the mean lifetimes were 3.33 and 1.02 ns in the absence and presence of the acceptor, respectively. From these numbers we obtain from the rate of hetero energy transfer $(k_{HT})^{-1} = 1.47$ ns. Using the corresponding numbers for the P_{fr}/P_r photoequilibrium we calculate $(k_{HT})^{-1} = 2.70$ ns. From the analysis of the homo energy transfer data we obtained $(k_{HT})^{-1} = 2.15$ ns. We conclude that the rate of homo and hetero energy transfer are of comparable magnitude. This is also what one would expect on the basis of the similar overlap integrals for the PEB/PEB and PEB/PCB pairs, if we assume furthermore that the κ^2 values for these pairs are similar as well. The fact that the rates of homo and hetero energy transfer from the two independent sets of experiments are qualitatively in agreement provides further evidence for energy transfer.

The effect of homo energy transfer on the anisotropy was analyzed with a powerlaw with $(k_{HT})^{-1} = 2.15$ ns and $n = 0.34$. The small value of n corresponds to a broad distribution of rate constants and is indicative of considerable heterogeneity. With these values for the mean rate constant k_{HT} and n, the distribution of rate constants was calculated. This allowed in turn the corresponding distribution of donor−acceptor distances to be calculated (*35*). Using the full width at half-height as the criterion for the width of the distribution, we obtained 44.0 Å $< R_{DA} <$ 62.3 Å with the maximum value at 51.3 Å. It is likely that this heterogeneity is not of structural origin but instead due to spectral shifts, as was recently suggested from single-molecule energy transfer experiments between the chromophores of the related cyanobacterial system phycoerythrocyanin (*36*).

The rotational correlation times differ significantly between Cph1 and Cph1Δ2 monomers and the Cph1 dimers. For Cph1Δ2 (58 kDa) at 0.25 μM, we observed the smallest time of 50 ns suggesting that it is indeed largely monomeric. For the Cph1 monomer (85 kDa), measured at high dilution, we obtained 62 ns, whereas for the Cph1 dimer (170 kDa) values between 85 and 110 ns were measured. These values are about what one expects for hydrated spheres of these molecular weights (*21*). Because of the short lifetime of PEB and the limited observation window of about 17 ns, the errors in these numbers are large. Therefore, and because of complications due to the nonspherical shape (*21*), these rotational correlation times cannot be recommended to monitor the dimerization of Cph1. We note that a rotational correlation time of 103 ns was observed for ANS labeled oat phytochrome (118 kDa) using phase fluorimetry (*37*).

Dilution of PEB/PEB dimers (Figure 7) led to a significant increase in anisotropy without a change in lifetime. These experiments indicate a decrease in homo energy transfer due to dimer dissociation and show that at concentrations below 10 μM, Cph1 occurs in a monomer/dimer equilibrium. This allowed us to estimate a dissociation constant of 5 μM from the concentration dependence of the anisotropy. To our knowledge, this is the first estimate of the dimer dissociation constant for a prokaryotic phytochrome. For plant phytochrome A, a 500 pM upper limit for the dissociation constant has been estimated (*18*). The intersubunit interactions are thus clearly much weaker in Cph1 dimers than in plant phytochrome dimers. One major difference between Cph1 (85 kDa) and plant phytochrome (124 kDa) is the absence of about 300 amino acids in the PAS module between the sensor and the transmitter modules. Thus, reduced subunit interaction in Cph1 might well be due in part to the absence of the PAS module and the associated contact area. Additional removal of the transmitter module, as in the deletion mutant Cph1Δ2, led to a further reduction in dimerization but did not abolish the association.

In previous work, the association of Cph1 was characterized by size-exclusion chromatography (*7*, *19*, *20*). Since these authors did not specify the Cph1 concentrations used in their experiments, their mutually contradictory results are difficult to evaluate and may not be compared directly to ours. The SEC experiments are in agreement concerning apo Cph1, which was shown to be predominantly monomeric (*19*, *20*). The Cph1 holoprotein, however, seems to be either in a 50:50 monomer/dimer equilibrium (*20*) or completely dimerized (*19*). Results with Cph1D apoprotein, a deletion mutant consisting of the first 490 amino acids from the N-terminus, indicate that this truncated protein is entirely monomeric (*20*). This is not necessarily in contradiction to our results with Cph1Δ2, which consists of the first 513 amino acids. Moreover, we investigated the Cph1Δ2 holoprotein. Discrepancies between the expected molecular weights and those deduced from the SEC mobilities have been attributed to a nonglobular shape or to interactions with the gel matrix (*7*, *19*, *20*). The conditions of ionic strength, concentration, and pH in the column may furthermore affect the dimerization equilibrium. Nevertheless, these results from SEC provide evidence for dimerization and suggest that chromophore binding leads to stronger association. The latter result is in line with the change in secondary structure observed upon chromophore binding in the far-UV CD spectrum (*20*). Our data analysis did not consider the possibility that the chromophore binding shifts the monomer/dimer equilibrium toward the dimer. Since our titration experiments were performed at concentrations well above the K_D, most of the phytochrome molecules were in the dimer state so that this effect can be neglected. Moreover, the residuals in Figure 5E show that our model provides an adequate description of our observations over the entire titration. With our experimental data there is therefore no need for a more refined model.

Our finding that energy transfer in full-length Cph1 dimers is stronger in the P_r than in the P_{fr} form is of great interest

since it may be related to the change in histidine kinase activity, which is larger in P_r than in P_{fr}. A structural change might bring the histidine kinase domains in the P_r dimer closer together thereby increasing the rate of transphosphorylation. This closer proximity may also affect the chromophore domains and lead to the observed increase in the rate of energy transfer. This result was obtained in hetero energy transfer experiments, which are difficult to analyze and interpret due to the multiple lifetimes. We note that the direction of the effect, more energy transfer in P_r, is consistent with the larger spectral overlap in this state. In related energy transfer experiments between a fluorescently labeled antibody to the N-terminus of oat phytochrome and the chromophore, a change in distance between donor and acceptor was observed upon photoconversion, partially compensating the difference in the spectral overlap (*38*).

Because of the isomerization and the associated orientation change of the PCB transition dipole moment, the κ^2 factor will probably also differ between P_r and P_{fr}. A substantial change of the transition dipole moment orientation between P_r and P_{fr} was detected by linear dichroism in pea (*39*) and oat (*40*, *41*) phytochrome. Since the related change in κ^2 is unknown in Cph1, it is not possible to interpret this observation further at this time in terms of a structural effect. We note that in the truncated deletion mutant Cph1Δ2 the opposite effect was observed: stronger energy transfer in P_{fr} despite the larger spectral overlap in P_r. It seems reasonable to assume that the change in κ^2 between P_r and P_{fr} is the same in Cph1 and Cph1Δ2, implying that there is a structural change that is reflected in the chromophore−chromophore distance. However, alternatively our results for Cph1Δ2 could be explained by a stronger dimerization of the P_{fr} form, as compared to the P_r form. This possibility is supported by recent experiments using the analytical ultracentrifuge, which indicated that the dissociation constant is much smaller in P_{fr} than in P_r (H. Strauss, and J. Hughes, unpublished results).

Similar energy transfer experiments as carried out here with Cph1 may also be feasible with plant phytochrome and could provide valuable information on structural changes and dissociation constants.

ACKNOWLEDGMENT

We thank Stefanie Krohn and Norbert Michael for purification of proteins and chromophores and Ulrike Alexiev for useful discussions.

REFERENCES

1. Hughes, J., Lamparter, T., Mittmann, F., Hartmann, E., Gärtner, W., Wilde, A., and Börner, T. (1997) *Nature 386*, 663−663.
2. Yeh, K. C., Wu, S. H., Murphy, J. T., and Lagarias, J. C. (1997) *Science 277*, 1505−1508.
3. Bhoo, S.-H., Davis, S. J., Walker, J., Karniol, B., and Vierstra, R. D. (2001) *Nature 414*, 776−779.
4. Davis, S. J., Vener, A. V., and Vierstra, R. D. (1999) *Science 286*, 2517−2520.
5. Lamparter, T., Michael, N., Mittmann, F., and Estaban, B. (2002) *Proc. Natl. Acad. Sci. U.S.A. 99*, 11628−11633.
6. Hughes, J., and Lamparter, T. (1999) *Plant Physiol. 121*, 1059−1068.
7. Lamparter, T., Mittmann, F., Gärtner, W., Börner, T., Hartmann, E., and Hughes, J. (1997) *Proc. Natl. Acad. Sci. U.S.A. 94*, 11792−11797.
8. Remberg, A., Lindner, I., Lamparter, T., Hughes, J., Kneip, C., Hildebrandt, P., Braslavsky, S. E., Gärtner, W., and Schaffner, K. (1997) *Biochemistry 36*, 13389−13395.
9. Van Thor, J. J., Borucki, B., Crielaard, W., Otto, H., Lamparter, T., Hughes, J., Hellingwerf, K. J., and Heyn, M. P. (2001) *Biochemistry 40*, 11460−11471.
10. Foerstendorf, H., Lamparter, R., Hughes, J., Gärtner, W., and Siebert, F. (2000) *Photochem. Photobiol. 71*, 655−661.
11. Sineshchekov, V., Hughes, J., and Lamparter, T. (1998) *Photochem. Photobiol. 67*, 263−267.
12. Sineshchekov, V., Koppel, L., Esteban, B., Hughes, J., and Lamparter, T. (2002) *J. Photochem. Photobiol. B 67*, 39−50.
13. Hübschmann, T., Börner, T., Hartmann, E., and Lamparter, T. (2001) *Eur. J. Biochem. 268*, 2055−2063.
14. Holzwarth, A. R., Venuti, E., Braslavsky, S. E., and Schaffner, K. (1992) *Biochim. Biophys. Acta 1140*, 59−68.
15. Sineshchekov, V. A. (1995) *Biochim. Biophys. Acta 1228*, 125−164.
16. Li, L., Murphy, J. T., and Lagarias, J. C. (1995) *Biochemistry 34*, 7923−7930.
17. Murphy, J. T., and Lagarias, J. C. (1997) *Curr. Biol. 7*, 870−879.
18. Edgerton, M. D., and Jones, A. M. (1993) *Biochemistry 32*, 8239−8245.
19. Lamparter, T., Esteban, B., and Hughes, J. (2001) *Eur. J. Biochem. 268*, 4720−4730.
20. Park, C.-M., Shim, J.-Y., Yang, S.-S., Kang, J.-G., Kim, J.-I., Luka, Z., and Song, P.-S. (2000) *Biochemistry 39*, 6349−6356.
21. Lakowicz, J. R. (1999) *Principles of Fluorescence Spectroscopy*, 2nd ed., Kluwer Academic/Plenum Publishers, New York.
22. Van der Meer, B. W., Coker, G., III, and Chen, S.-Y. (1994) *Resonance Energy Transfer: Theory and Data*, VCH Publishers, New York.
23. Karolin, J., Fa, M., Milczynska, M., Ny, T., and Johansson, L. B.-Å. (1998) *Biophys. J. 74*, 11−21.
24. Johansson, L. B.-Å., Edman, P., and Westlund, P.-O. (1996) *J. Chem. Phys. 105*, 10896−10904.
25. Tanaka, F. (1998) *J. Chem. Phys. 109*, 1084−1092.
26. Tanaka, F., and Mataga, N. (1979) *Photochem. Photobiol. 29*, 1091−1097.
27. Nakasako, M., Wada, M., Tokutomi, S., Yamamoto, K. T., Sakai, J., Kataoka, M., Tokunaga, F., and Furuya, M. (1990) *Photochem. Photobiol. 52*, 3−12.
28. Jones, A. M., and Erickson, H. P. (1989) *Photochem. Photobiol. 49*, 479−483.
29. Heyn, M. P. (1989) *Methods Enzymol. 172*, 462−471.
30. Mielke, T., Alexiev, U., Gläsel, M., Otto, H., and Heyn, M. P. (2002) *Biochemistry 41*, 7875−7884.
31. Austin, R. H., Beeson, K., Eisenstein, L., Frauenfelder, H., Gunsalus, I. C., and Marshall, V. P. (1974) *Phys. Rev. Lett. 32*, 403−405.
32. Hennig, L., and Schäfer, E. (2001) *J. Biol. Chem. 276*, 7913−7918.
33. West, A. H., and Stock, A. M. (2001) *Trends Biochem. Sci. 26*, 369−376.
34. Stock, A. M., Robinson, V. L., and Goudreau, P. N. (2000) *Annu. Rev. Biochem. 69*, 183−215.
35. Haran, G., Haas, E., Szpikowska, B. K., and Mas, M. T. (1992) *Proc. Natl. Acad. Sci. U.S.A. 98*, 11764−11768.
36. Zehetmayer, P., Hellerer, T., Parbel, A., Scheer, H., and Zumbusch, A. (2002) *Biophys. J. 83*, 407−415.
37. Sarkar, H. K., Moon, D.-K., Song, P.-S., Chang, T., and Yu, H. (1984) *Biochemistry 23*, 1882−1888.
38. Farrens, D. L., Cordonnier, M.-M., Pratt, L. H., and Song, P.-S. (1992) *Photochem. Photobiol. 56*, 725−733.
39. Tokutomi, S., and Mimuro, M. (1989) *FEBS Lett. 255*, 350−353.
40. Ekelund, N. G. A., Sundquist, C., Quail, P. H., and Vierstra, R. D. (1985) *Photochem. Photobiol. 41*, 221−223.
41. Sundquist, C., and Björn, L. O. (1983) *Photochem. Photobiol. 37*, 69−75.

BI026946Y